Highly transparent bismuth oxide thin films deposition: morphology - optical properties correlation studies

S. CONDURACHE-BOTA[a*], V. TIRON[b], M. PRAISLER[a]
[a] *"Dunărea de Jos" University of Galati, Faculty of Sciences and Environment, 111 Domneasca Street, 800201, Galati, Romania*
[b] *Alexandru Ioan Cuza University, Faculty of Physics, IPARC – Iasi Plasma Advanced, Research Center, 11 Carol I Blvd., 700506, Iasi, Romania*

Bismuth oxide thin films have proved to exhibit properties that recommend them for a large area of applications, from Optoelectronics to humidity and other oxygen-containing gases sensors. Still, scarce references have been found so far as concerning high optically-transmitting bismuth oxide thin films. This paper reports on such highly transparent bismuth oxide films, with over 60 % transmittance within the 500-1100 nm spectral range. Pulsed laser deposition was the method of choice for the preparation of the films. It is also showed here that the morphology plays an important role concerning many optical properties of the resulting films, from the transmittance, to the reflectivity, to the absorption coefficient and as related to the refractive index, respectively. The deposition conditions change the roughness of the films which, in turn, affects the optical parameters.

(Received July 20, 2015; accepted September 9, 2015)

Keywords: Thin films, Bismuth oxide, Roughness, Atomic Force Microscopy, Optical parameters

1. Introduction

The breakthrough of LASER effect and devices represented a turning point both for science and technology. Thus, coherent, monochromatic and possible high energy laser radiation quickly found its uses in Metrology, Telecommunications, Spectroscopy, Medicine, Computers, Music, Industry (cutting, welding, etc.) and even for barcode scanners in stores and in the Entertainment Industry, for its impressive visual effects [1-5]. Not long after the development of Q-switched lasers in the 1980's, which proved capable of delivering laser pulses of extremely high energy, a novel thin film deposition technique was achieved, called pulsed laser deposition (PLD). This technique makes use of the capability to concentrate high energy laser beams on small volumes of material, which can be removed (ablated) this way from the bulk in controllable quantities, such that the extracted material deposits on the nearby surfaces. The material ablated from the laser target further interacts with the laser pulses, such that it forms a supersonic jet of hot and inherently, partially ionized particles giving rise to a visible plasma with specific shape, called 'plume', due to its feather-like shape (see Fig. 1a). The plasma visible radiation is due to the fluorescence and recombination processes happening within it.

If a substrate with good adherence is placed opposite to the target, the ablated particles would deposit on it in a layer whose thickness mainly depends on material ablation efficiency, on compatibility between the target material and the substrate and on the number of laser pulses sent on the target [2-7].

The material to be ablated must be pressed in a dense target (see Fig. 1b), such the material removal upon laser impact would be as uniform and smooth as possible. Thus, no big chunks of substance (particulate matter) would be snatched from the target, since these would result in a bad, inhomogeneous and non-uniform deposition on the substrate of choice. In order to insure the uniform deposition of material on a substrate, a compromise must be made for the target impact area of the laser pulses, such that, on one hand, it would be large enough to ensure sufficient material removal and, on the other hand, it would be small enough not to allow for particulates to be removed from the target, that would damage the resulting films deposited on the substrate. Fig. 1c presents such a target impact area of 0.60 mm^2, as used in the case of the films analysed here. Such a technique proved efficient for the ablation and subsequent deposition as thin or thicker films of various types of materials, including those with high melting point, such as the refractory oxides [1,7-9].

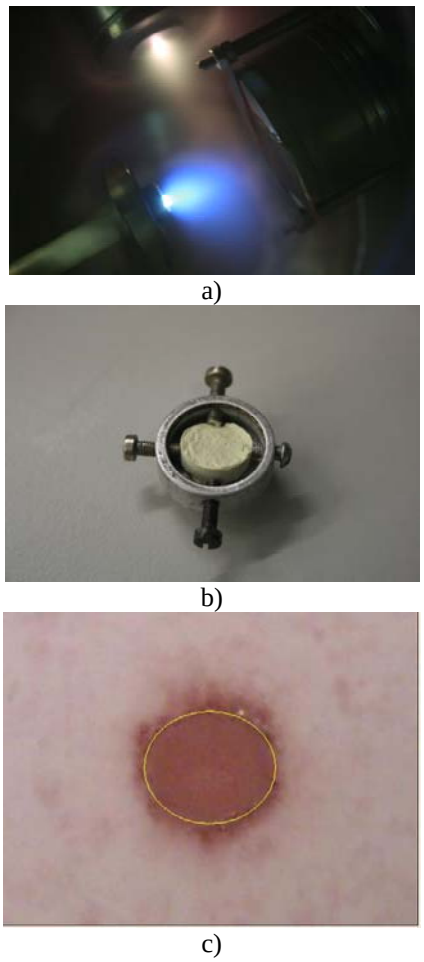

Fig. 1 Specific PLD images of: a). the laser plume (the blue one, from the bottom) of ablated material, together with the whitish oxygen plasma (from the top) induced by a radiofrequency discharge within the ablation chamber; b). a bismuth target pressed in coin shape and mounted in the device to be placed into the ablation chamber; c). the impact area of the laser pulses on the target in Fig. 1b, in false colour.

A specific advantage of the PLD technique consists in the possibility to introduce various gas flows in the ablation chamber, such that it would interact with the material ablated from the target. Moreover, in the case of an oxygen flow, a radiofrequency (RF) discharge can induce its plasma state (the whitish plasma from the top to bottom in Fig. 1b), making oxygen more reactive with the ablated material, thus oxidizing it more effectively [2,3,10].

This is the case with the films studied within this paper. Thus, pure bismuth target were pulsed laser ablated within an RF-induced oxygen plasma, such that bismuth oxide films were deposited on pure bismuth substrates. Bismuth was the material of choice because its trioxide proved valuable for various optical, electronic and optoelectronic applications, given its high energy bandgap, between 2.31 – 3.55 eV and due to its large range of values for the refractive index: 1.6 – 3.6 in NIR-VIS-UV [11-13]. The optical properties of the resulting films were studied along with their morphology, since the latter strongly influence the former and since this information is fundamental for optoelectronic and gas sensing applications of thin films.

2. Experimental

Radiofrequency-assisted pulsed laser deposition with 193 nm wavelength laser pulses and 10 Hz repetition frequency were used for the ablation of pure bismuth coin-shaped targets pressed at an industrial press. The UV laser wavelength was chosen since in this spectral range the ablation efficiency is higher due to the lower target reflectivity and inherent stronger absorption. One hundred minutes of target ablation was performed for each deposited film, such that 60 000 laser pulses were used for material removal. The oxygen flow was set at 100 cm^3 per minute and 150 W was the power of its radiofrequency discharge.

The substrates of choice were microscope glass slides. Their temperature was set at different values between 27^0C and 600^0C, since it is a known fact that the substrate temperature (denoted as t_S in the following) plays a key role during material deposition, changing the distribution of depositing molecules as their thermal energy increases with increasing substrate temperature and, thus, it influences the properties of the resulting films [14-16].

Film thickness measurements were done by means of the multiple-beam Fizeau fringe method with a white light-operated *MII-4 Linnik* interferential microscope.

The optical analysis was performed between 200 and 1100 nm by means of a single beam *Perkin Elmer Lambda 35* spectrophotometer, operating in air, at normal incidence. Air was the reference for the optical transmittance measurements, while a high-reflecting mirror was used as reference for the reflectance.

The absorption coefficient, α of the films was computed as [17]:

$$\alpha = \frac{1}{d} \cdot \ell n\left(\frac{1}{T}\right) \quad (1)$$

with d being the thickness of a certain film and T its transmittance for a specific wavelength.

In order to infer the refractive index of the films, their absorption index $\bar{k}$ was found as [18]:

$$\bar{k} = \frac{\alpha \cdot \lambda}{4\pi} \quad (2)$$

with λ denoting the wavelength of the incident radiation.

Thus, by also using the reflectance, R of each film, its refractive index was computed as [19]:

$$n = \frac{1+R+\sqrt{(1+R)^2-(1-R)^2\cdot\left(1-\bar{k}^2\right)}}{1-R} \quad (3)$$

The morphology analysis was performed by means of Atomic Force Microscopy (AFM), by using a *NT-MDT Solver Pro-M* AFM Microscope, with 2 nm horizontal resolution and 0.1 nm vertical resolution. Several specific morphological parameters were inferred from the two-dimensional (2D) AFM images: average peak height, $z_{average,}$ maximum peak height, R_p, mean roughness, R and root mean square roughness (RMS), the last two features being given by [20]:

$$R_a = \frac{1}{n}\cdot\sum_{i=1}^{n}\left|z_i-\bar{z}\right| \quad (4)$$

$$RMS = \sqrt{\frac{1}{n}\cdot\sum_{i=1}^{n}\left|z_i-\bar{z}\right|^2} \quad (5)$$

where n denotes the number of scanned and measured points within the 2D AFM image, z_i represent the height of each peak in the image, while $\bar{z}$ represents the average peak height.

3. Results and discussion

Fig. 2 and 3 present the optical transmittance and optical reflectance spectra of five types of bismuth oxide thin films deposited by RF-PLD at substrate temperatures up till 600^{0}C. The transmittance factor surpasses 60 % in the Visible and Near-infrared, especially above 500 nm, for all five types of investigated films, as only some have found so far, by using different deposition techniques than the one presented here [21,22]. The highest transmittance in the present study corresponds to the film deposited at t_S=500^{0}C all along the investigated spectral range. The slight wave-like shape of the transmittance spectra is an indication of the good film uniformity giving rise to multiple interferences of the radiations resulting from the multiple reflections at the interfaces air-film and film-substrate. Still, the wave-like aspect of the transmittance was too weak to apply Swanepoel's algorithm for the computation of the relevant optical parameters of the films [23].

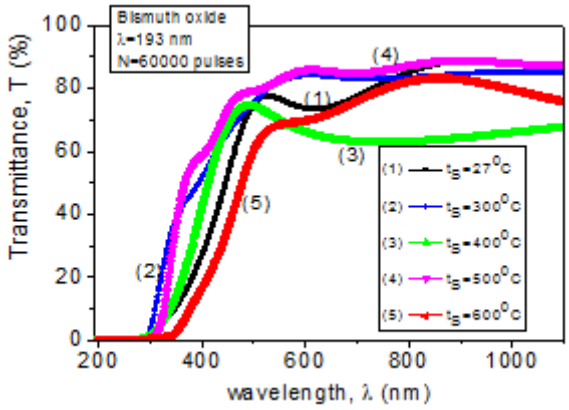

Fig. 2 The transmittance spectra of the films under study for the UV-VIS-NIR spectral range

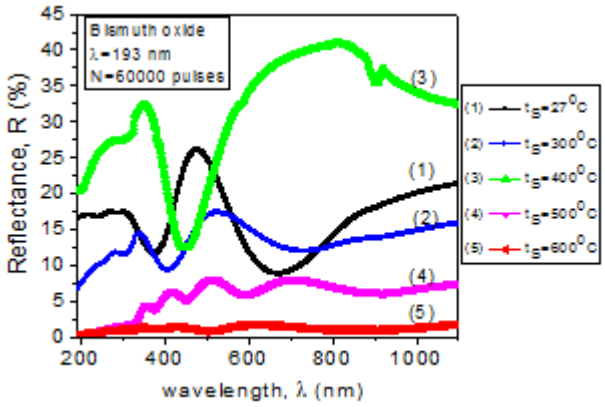

Fig. 3 The reflectance spectra of the films under study for the UV-VIS-NIR spectral range

As far as the reflectance of the films is concerned, it largely varies from less than 2 % for the film deposited at 600^{0}C to almost 41 % for the film with t_S=400^{0}C, the latter being the highest reflector of all the investigated films for wavelengths above 500 nm.

Following the algorithm described above, the absorption coefficient and the refractive index of the films were computed, since they represent key optical parameters, valuable for inferring both optical and optoelectronic applications of the analysed films. Fig. 4 presents the optical absorption spectra of the investigated bismuth oxide films, while Fig. 5 shows the wavelength dependence of the refractive index of each studied film. As expected, the film deposited at 500^{0}C has the lowest absorption, since it exhibits the highest transmittance of all the investigated films, while the best absorber for λ> 500 nm is the film with t_S=400^{0}C, whereas for wavelengths between 400 and 500 nm, the highest absorption coefficient is found for the film deposited at 600^{0}C, up till 5 μm^{-1}.

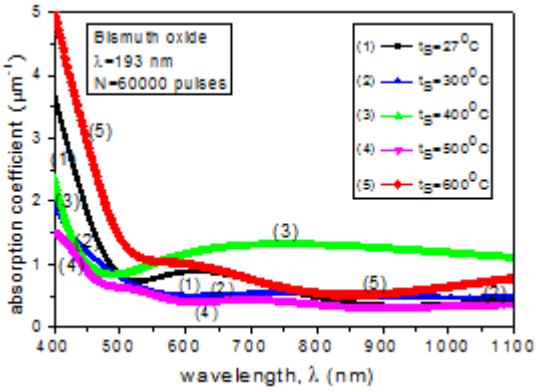

Fig. 4 The optical absorption spectra of the analysed bismuth oxide films

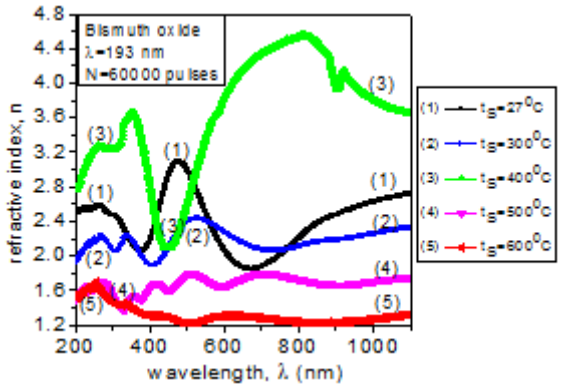

Fig. 5 The wavelength-dependence of the refractive index of the bismuth oxide films under study

The refractive index of the films varies from 1.2 to 4.6, as obtained by Leontie &collaborators and by some of the co-authors of the present paper, by using different deposition techniques [13,14,17]. In this study, the highest values of the refractive index are reached above 500 nm for the film with the highest corresponding reflectance, i.e. the film deposited at 400^{0}C. There are some narrow spectral ranges with abnormal dispersion for the refractive index for all investigated films.

As stated above, the morphology of a thin film has an essential influence on its optical properties, since grain sizes and distribution mainly determine film reflectance. But the surface roughness is also extremely relevant for gas sensing applications, since as a material has a higher effective contact area with the gas to be detected, its gas sensitivity would be higher. This effective contact area is given by both the grain size, but also by the peaks and valleys distribution, such that several types of roughness parameters must be inferred as related to gas sensing investigations, but also when the optical properties are concerned [24]. Fig. 6 presents the two-dimensional AFM images of the investigated bismuth oxide thin films, at 1 μm x 1 μm scale, while the side scale shows the coloured legend of the peaks heights, also showing the highest and the smallest measured peaks.

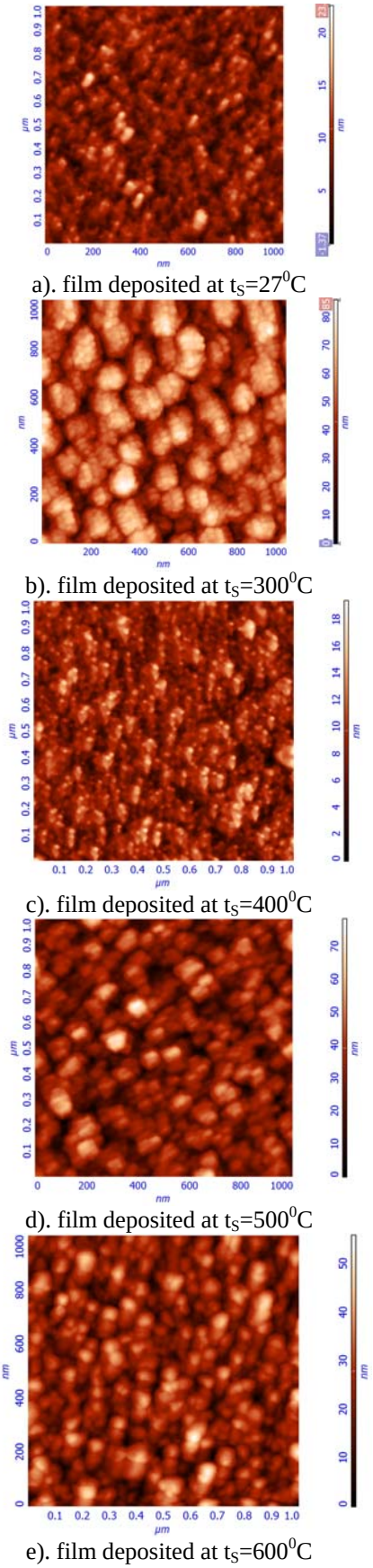

a). film deposited at t_S=27^{0}C

b). film deposited at t_S=300^{0}C

c). film deposited at t_S=400^{0}C

d). film deposited at t_S=500^{0}C

e). film deposited at t_S=600^{0}C

Fig. 6 The 2D Atomic Force Microscopy images of the studied bismuth oxide films

It can be noticed that the surfaces of all the investigated films exhibit an uniform distribution of crystalline grains, with columnar shape for the films deposited at t_S = 27^{0}C, 400 ^{0}C and 600 ^{0}C, while the film with t_S = 300^{0}C contains cauliflower-like grains.

Table 1 presents representative roughness parameters of the analysed bismuth oxide thin films, as inferred from the 2D AFM images, along with their thickness, as computed by white-light interferometry. One can easily noticed that the films grew thicker as the substrate temperature was set at higher values. As for the roughness parameters, their highest values are noticed for the film deposited at t_S=300^{0}C, with cauliflower-like grains, in spite of its intermediate thickness. Thus, grains as high as 85 nm were measured on the surface of this film as compared to less than 20 nm for the highest grains of the film deposited on glass maintained at t_S=400^{0}C. High grains were also measured for the film with t_S=500^{0}C, while the films with t_S=27^{0}C and 400^{0}C present similar roughness. The RMS of each film surpasses 730 nm, while the mean roughness stays below 12 nm.

Table 1 Representative roughness parameters and thickness of the analysed bismuth oxide thin films

Substrate temperature, t_S (^{0}C)	**Film thickness, d (μm)**	**Average peak height, $z_{average}$ (nm)**	**Mean roughness, R_a (nm)**	**RMS (nm)**	**Max. height, R_p (nm)**
27	0.355	7.86	2.08	733.51	22.54
300	0.519	*47.13*	*11.74*	*833.27*	*85.88*
400	0.559	8.30	1.93	751.38	19.38
500	0.719	30.63	8.45	742.17	78.06
600	0.836	23.54	6.32	758.32	55.70

By correlating the optical data with the morphology of the films it can be seen that the highest transparency for λ > 500 nm is obtained in the case of the film with t_s = 500^{0}C, having round and horizontally-oriented crystalline grains. For the same spectral range, the strongest absorption, the highest reflectance and highest refractive index (>2.8) are found for the film with $t_S = 400^0\,C$, with the thinnest columnar grains. The cauliflower-like film has intermediate optical parameters, but, due to its porous morphology, it is the most susceptible of high gas sensitivity. The lowest mean roughness and the maximum height are exhibited by the film with t_s = 400^{0}C, which presents the highest reflectance over most VIS and in the NIR.

4. Conclusions

The morphology and fundamental optical parameters were investigated for radiofrequency-assisted pulsed laser deposited bismuth oxide thin films on glass substrates maintained at temperatures ranging from 27^{0}C till 600^{0}C. The ablated bismuth oxidized, while depositing, with the oxygen inside the deposition chamber. The gas was turned to plasma by a radiofrequency discharge, in order to make it more reactive with the target material.

It was found that both the morphology and the optical parameters of the films change significantly with changing substrate temperature, being inter-correlated.

The crystalline grains grew uniformly distributed either as columns or as nanometric cauliflowers, in the latter case the surface being the roughest of all the analyzed films, with RMS as high as 833.27 nm.

High transparency was noticed above 500 nm for all the films, but especially high transmittance, above 80 % was reached by the film deposited at 500^{0}C, whose surface presents round and horizontally-oriented crystalline grains. Meanwhile, the film deposited at 400^{0}C substrate temperature has the thinnest columnar grains, but the highest absorption, reflectance and refractive index above 550 nm.

Thus, the film deposited at t_S=500^{0}C is recommended for transparent electronics in the Visible and Near-Infrared, while the film with the highest potential for gas sensitivity due to its specific porous, cauliflower-like surface is the one deposited at t_S=300^{0}C.

Acknowledgements

The work has been funded by the Sectoral Operational Programme Human Resources Development 2007-2013 of the Ministry of European Funds through the Financial Agreement POSDRU/159/1.5/S/132397.

References

[1] R. Eason, Pulsed laser deposition of thin films: applications-led growth of functional materials, John Wiley & Sons Inc., New York (2007).
[2] H.–U. Krebs, M. Weisheit, J. Faupel, E. Suske, T. Scharf, C. Fuhse, M. Stormer, K. Sturm, M. Seibt, H. Kijewski, D. Nelke, E. Panchenko, M. Buback, Adv. Solid State Phys. **43**, 505 (2003).
[3] E. Morintale, C. Constantinescu, M. Dinescu, Physics AUC **20**(I), 43 (2010).
[4] M. N. R. Ashfold, F., Claeyssens, G. M. Fuge, S. J. Henley, Chem. Soc. Rev. **33**, 23 (2004).
[5] D. S. Wu, David J. Richardson, R. Slavík, Optica **2**, 18 (2015).
[6] M. Popescu, L. Diamandescu, A. Velea, J. Intense Pulsed Lasers Appl. Adv. Phys. **1**(1), 21 (2011).
[7] J. S. Horwitz and J. A. Sprague, Film Nucleation and Film Growth in Pulsed Laser Deposition of Ceramics *in* Pulsed Laser Deposition of Thin Films, D. B. Chrisey and G. K. Hubler (editors), John Wiley & Sons Inc., New York (1994).
[8] R. Bazavan, L. Ion, G. Socol, I. Enculescu, D. Bazavan, C. Tazlaoanu, A. Lorinczi, I.N. Mihailescu, M. Popescu, S. Antohe, J. Optoelectron. Adv. Mater., **11**(4), 425 (2009).
[9] A. Lorinczi, F. Sava, A. Stanoiu, C.E. Simion, G. Socol, I.N. Mihailescu, M. Popescu, J. Optoelectron. Adv. Mater. **9**(11), 3489 (2007).
[10] C. Gheorghies, S. Condurache-Bota, M. Dinescu, C. Constantinescu, N. Cazacu, Optoelectron. Adv. Mater. - Rapid Commmun. **2**(9), 569 (2008).
[11] C.M.B. Hincapié, M.J.P. Cárdenas, J.E.A. Orjuela, E.R. Parra and J.J.O. Florez, Dyna, **176**, 139 (2012).
[12] L. Leontie, J. Optoelectr. Adv. M. **8**(3), 1221 (2006).
[13] L. Leontie, M. Caraman, A. Visinoiu, G. I. Rusu, Thin Solid Films **473** (2), 230 (2005).
[14] S. Condurache-Bota, N. Tigau, A. P. Râmbu, G. G. Rusu, G. I. Rusu, Appl. Surf. Sci. **257**, 10545 (2011).
[15] B. A. Mansour, H. Shaban, S. A. Gad, Y. A. El-Gendy, A. M. Salem, J. Ovonic Res. **6**(1), 13 (2010).
[16] M. Sreemany, A. Bose, S. Sen, Physica B, **405,** 85 (2010).
[17] L. Leontie, M. Caraman, M. Delibas, G. I. Rusu, Mater. Res. Bull. **36 (9)**, 1629 (2001).
[18] M. Y. Nadeem, W. Ahmed, Turk. J. Phys. **24,** 651 (2000).
[19] F. Yakuphanoglu, M. Durmus, M. Okutan, O. Köysal, V. Ahsen, Physica B: Cond. Matter. **373** (2), 262 (2006).
[20] B.Rajesh Kumar, T. Subba Rao, Dig. J. Nanomater. Bios. **7**(4), 1881 (2012).
[21] R. B. Patil, R. K. Puri, V. Puri, Appl. Surf. Sci. **253**, 8682 (2007).
[22] R. A. Ismail, e-J. Surf. Sci. Nanotech. **4**, 563 (2006).
[23] R. Swanepoel, J. Phys. E: Sci. Instrum., **16,** 1214 (1983).
[24] H. Farahani, R. Wagiran, M. N. Hamidon, Sensors **14,** 7881 (2014).

*Corresponding author: scondurache@ugal.ro